RadioGraphics

Between a Rock and a Hard Place: Clinical and Imaging Features of Vascular Compression Syndromes[1]

Ruth Eliahou, MD • Jacob Sosna, MD • Allan I. Bloom, MD

Vascular compression syndromes are caused by the entrapment of vessels between rigid or semirigid surfaces in a confined anatomic space. Chronic entrapment may lead to arterial ischemia and embolism, venous stasis and thrombosis, and hematuria. These syndromes are usually seen in otherwise healthy young patients, among whom underdiagnosis is common. Most occurrences of vascular compression are associated with an underlying anatomic abnormality. In a small percentage of cases, other contributing factors, including repetitive microtrauma, may cause pathologic changes leading to the onset of pain and other symptoms of vascular and neural compression. Hence, the diagnosis must be based on both clinical and radiologic findings. Because some cases of vascular entrapment become symptomatic only when specific physical maneuvers are performed, dynamic diagnostic imaging methods are especially useful. Digital subtraction angiography has been the mainstay of imaging-based diagnosis for most vascular compression syndromes, but other methods (eg, color Doppler ultrasonography, computed tomographic angiography, and magnetic resonance angiography) are used with increasing frequency for initial diagnostic evaluation. Because vascular compression syndromes are caused by the external compression of vessels, endoluminal treatment alone is rarely adequate and surgical decompression is likely to be required for optimal and durable clinical benefit. Supplemental material available at *http://radiographics.rsna.org/lookup/suppl/doi:10.1148/rg.321115011/-/DC1*.

ONLINE-ONLY CME

This article meets the criteria for ***AMA PRA Category 1 Credit™****. See www.rsna.org/education/rg_cme.html*

LEARNING OBJECTIVES

After completing this journal-based CME activity, participants will be able to:

- Recognize the imaging findings associated with various arterial and venous vascular compression syndromes.
- Discuss the diagnostic and therapeutic uses of angiography in each syndrome.
- Describe the anatomic abnormality associated with each syndrome.

TEACHING POINTS

See last page

Abbreviations: DSA = digital subtraction angiography, LCIV = left common iliac vein, RCIA = right common iliac artery, TOS = thoracic outlet syndrome

RadioGraphics 2012; 32:E33–E49 • **Published online** 10.1148/rg.321115011 • **Content Codes:** IR VA

[1]From the Department of Radiology, Hadassah–Hebrew University Medical Center, P O Box 12000, Jerusalem, Israel 91120 (R.E., J.S., A.I.B.), and Department of Radiology, Beth Israel Deaconess Medical Center, Harvard University School of Medicine, Boston, Mass (J.S.). Recipient of a Cum Laude award for an education exhibit at the 2009 RSNA Annual Meeting. Received January 26, 2011; revision requested April 18 and received September 20; accepted September 28. For this journal-based CME activity, the authors, editor, and reviewers have no relevant relationships to disclose. **Address correspondence to** A.I.B. (e-mail: *allan@hadassah.org.il*).

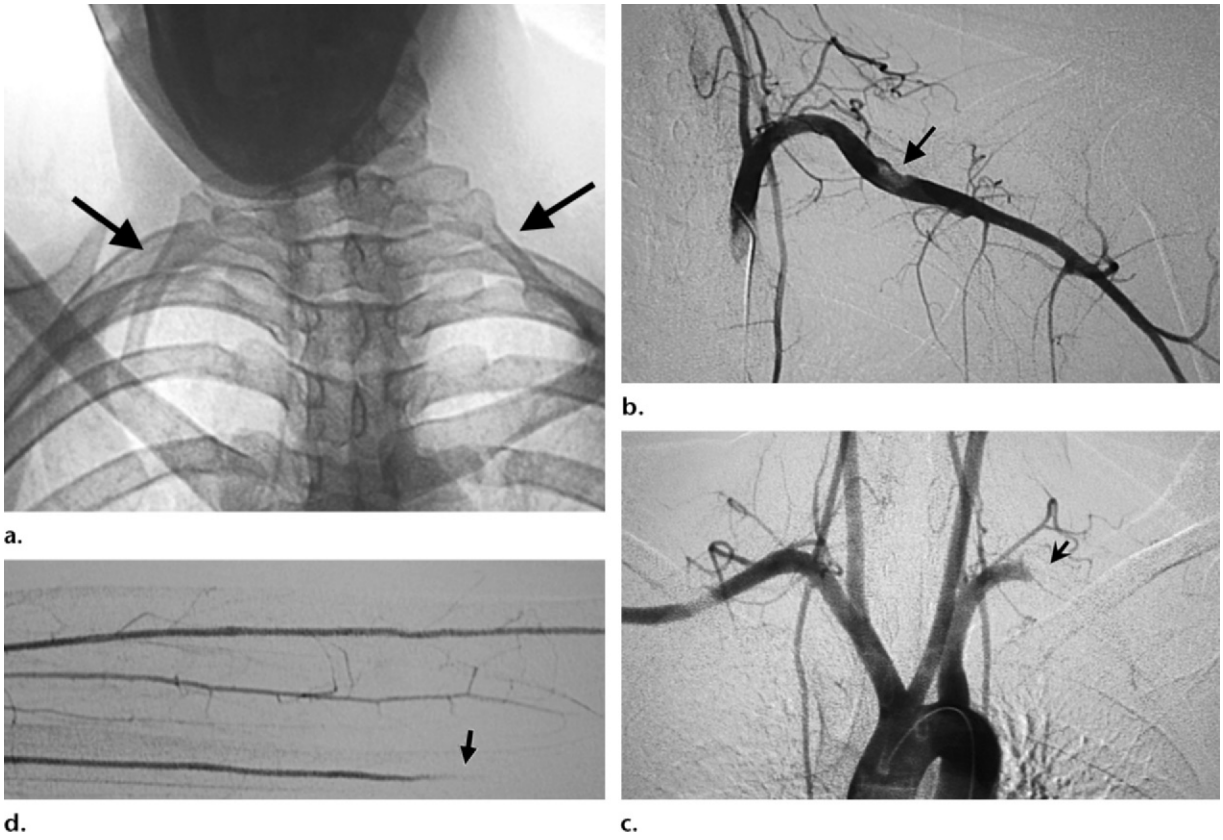

Figure 1. TOS due to arterial compression in a 20-year-old woman with acute left arm pain that intensified with exercise. **(a)** Radiograph shows bilateral cervical ribs (arrows). **(b)** Arteriogram obtained at DSA with the arm in a neutral position shows a thrombus (arrow) with irregularity and aneurysmal dilatation of the left subclavian artery. **(c)** Arch aortogram obtained at DSA with elevation and abduction of the arm shows complete left subclavian artery occlusion (arrow). **(d)** Arteriogram obtained at DSA shows embolism (arrow) of the distal left ulnar artery.

Introduction

Vascular compression syndromes are clinical entities caused by the entrapment of one or more blood vessels between rigid or semirigid surfaces in a confined anatomic space. Although they occur infrequently (less than 1% of the general population are affected), they may cause hemodynamically significant disease, including arterial ischemia and embolism, venous stasis and thrombosis, and hematuria in young, otherwise healthy patients.

Diagnosis of vascular compression syndromes is based on a comparison of clinical and imaging findings (1). The most commonly used imaging techniques are noninvasive and include color Doppler ultrasonography (US), computed tomographic (CT) angiography and venography, and magnetic resonance (MR) angiography and venography. However, digital subtraction angiography (DSA) continues to play a major role in the diagnosis and treatment of many of these syndromes.

The article surveys a spectrum of arterial and venous compression syndromes, including thoracic outlet syndrome (TOS), Paget-Schroetter syndrome (effort thrombosis), quadrilateral space syndrome, median arcuate ligament syndrome (celiac artery compression syndrome), nutcracker syndrome (renal vein entrapment syndrome), May-Thurner syndrome (left common iliac vein [LCIV] compression syndrome), and popliteal artery entrapment syndrome. The clinical and diagnostic features and pathophysiology of specific compression syndromes are discussed, and optimal methods for their imaging-based diagnosis and management are described. The characteristic imaging findings of each syndrome are described in detail.

Thoracic Outlet Syndrome

TOS is a neurovascular syndrome caused by compression of the subclavian vessels and brachial plexus in the narrow thoracic outlet area. There are three distinct types of TOS: neurogenic, arterial, and venous (Figs 1, 2), depending on what anatomic structure is compressed (2). Compression of the brachial plexus occurs in 95% of cases, whereas the subclavian vein is compressed in 4%, and the subclavian artery, in 1% (3).

Teaching Point

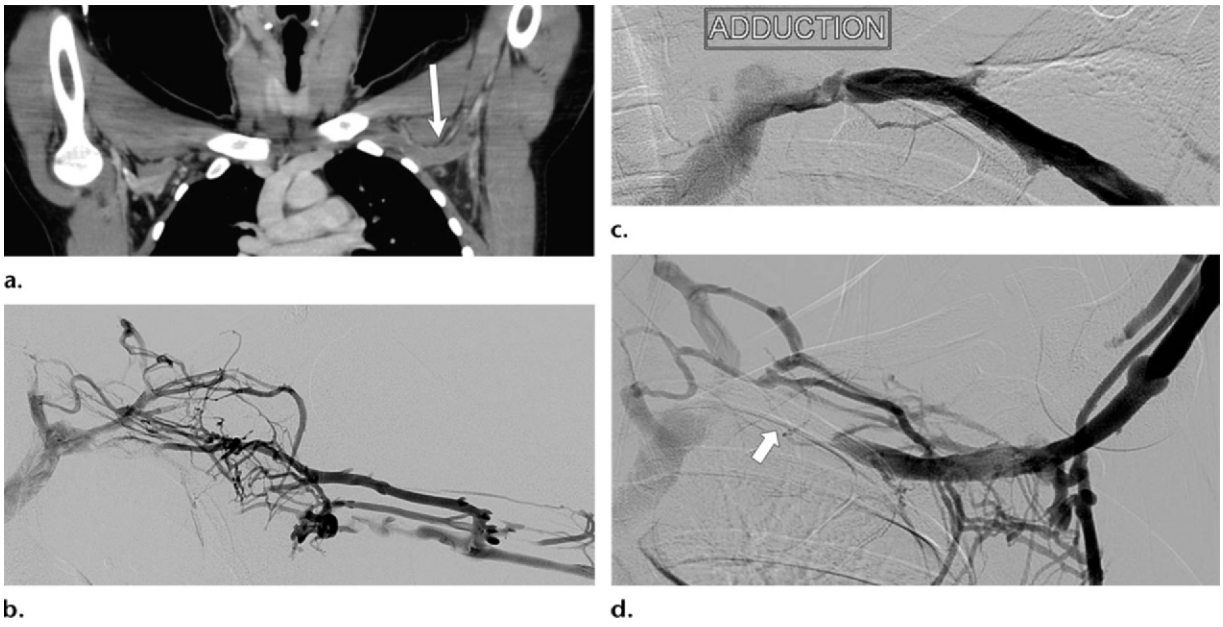

Figure 2. TOS due to venous compression (Paget-Schroetter syndrome) in a 16-year-old swimmer with a 1-week history of swelling and cyanosis in the left arm. **(a)** CT angiogram demonstrates left subclavian and axillary vein thrombosis (arrow). **(b)** Venogram obtained at DSA with the arm abducted 90° shows left axillary and subclavian vein thrombosis with multiple venous collaterals. **(c)** Venogram obtained at DSA with the arm adducted, 24 hours after venous catheterization and thrombolysis, shows a patent irregular subclavian vein with an abrupt severe stenosis in the costoclavicular space. **(d)** Venogram obtained at DSA after thrombolytic therapy shows subclavian vein occlusion (arrow), a typical feature of TOS, when the arm is hyperabducted.

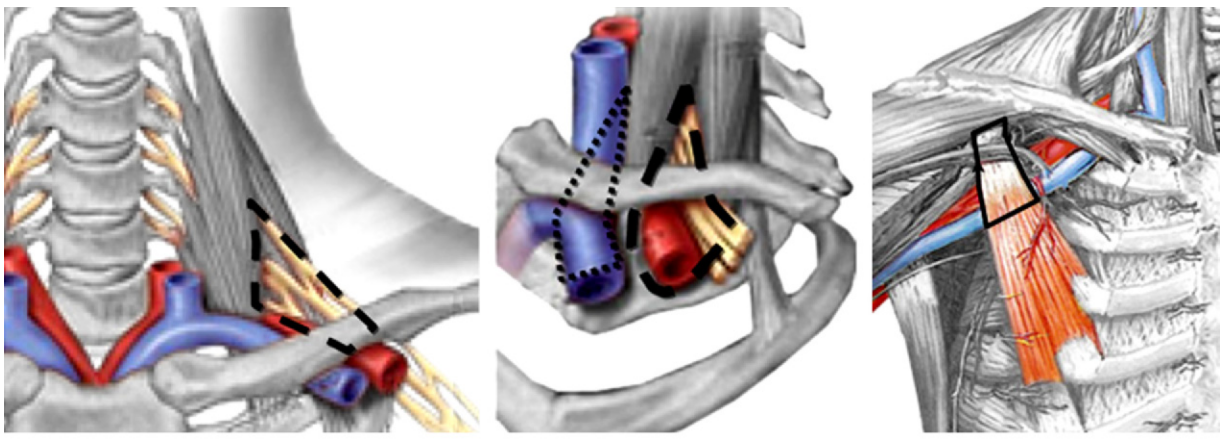

Figure 3. The thoracic outlet encompasses three anatomic spaces: the interscalene triangle, costoclavicular triangle, and retro–pectoralis minor space. **(a, b)** The interscalene triangle (dashed line in **a** and **b**), the farthest medial space, is bordered by the anterior scalene muscle anteriorly, the middle scalene muscle posteriorly, and the first rib inferiorly, and is transected by the subclavian artery and three divisions of the brachial plexus. The costoclavicular triangle (dotted line in **b**) is bordered by the middle third of the clavicle superiorly, the subclavian muscle anteriorly, and the first rib and scalene muscle posteriorly. **(c)** The retro–pectoralis minor space (solid line), the farthest lateral of the three spaces, is located beneath the coracoid process and is bordered by the pectoralis minor anteriorly, the subscapularis muscle posteriorly and superiorly, and the anterior chest wall posteriorly and inferiorly. TOS may be caused by musculoskeletal compression of the vessels and nerves within these spaces.

Anatomy

The thoracic outlet is located above the first rib and behind the clavicle. It includes three different anatomic spaces—the interscalene triangle, the costoclavicular space, and the retro–pectoralis minor space (1). The interscalene triangle, the most medial space, is bordered by the anterior scalene muscle anteriorly, the middle scalene muscle posteriorly, and the medial surface of the first rib inferiorly (Fig 3a). The subclavian artery

and the three divisions of the brachial plexus pass through it.

The second passageway is the costoclavicular triangle, which is bordered superiorly by the middle third of the clavicle, anteriorly by the subclavius muscle, and posteriorly by the first rib and middle scalene muscle (Fig 3b). The subclavian vein passes at the anterior aspect of this space, with the subclavian artery and the three cords of the brachial plexus located immediately posterior to it.

The retro–pectoralis minor space, also called the subcoracoid space, is the most lateral of the three and is located beneath the coracoid process. Its borders are the pectoralis minor muscle anteriorly, the subscapularis muscle posteriorly and superiorly, and the anterior chest wall posteriorly and inferiorly (Fig 3c). This space contains the axillary vessels and the three cords of the brachial plexus, which divide into five terminal branches.

Pathophysiology

Teaching Point

Even with the arm at rest, anatomic anomalies may result in narrowing of the thoracic outlet, a condition that may be exacerbated during physical maneuvers such as abduction of the arm. Elevation of the arm narrows the costoclavicular space and retro–pectoralis minor space in particular, with less effect on the interscalene triangle (4,5).

Vascular compression is most frequent in the costoclavicular space and less common in the interscalene triangle, whereas neurologic compression occurs with equal frequency in the costoclavicular space and the interscalene triangle (4). The retro–pectoralis minor space has rarely been reported as a site of compression (1).

The main causes of abnormal narrowing of the various thoracic outlet compartments are classified as either anatomic or posttraumatic. Anatomic sources of compression include cervical ribs, which occur in less than 1% of the general population (6), an elongated transverse process of the C7 vertebra, congenital fibromuscular bands, and aberrant scalene muscle anatomy (eg, hypertrophy of the anterior scalene or pectoralis minor muscles, a common origin of the anterior and middle scalene muscles, passage of the brachial plexus through the substance of the anterior scalene muscle, and supernumerary scalene muscles). Posttraumatic causes include first rib or clavicle fractures with excessive callus, scarring, and posttraumatic or surgical adhesions. Narrowing can also be caused by poor posture of the shoulder girdle with "drooping shoulder" and increased acromioclavicular descent.

The lack of an objective test allowing definitive confirmation of the diagnosis of TOS causes uncertainty regarding its true prevalence, with estimates ranging from 0.3% to 8% of the U.S. population (3,7). Those affected are typically women between the ages of 20 and 40 years (female-to-male ratio, 3–4:1) (8).

Symptoms and Signs

TOS is a dynamic syndrome with symptoms that usually manifest during elevation and abduction of the arm, particularly with sustained movement such as occurs while reaching for objects overhead, painting, or lifting. Symptoms vary according to the focus of compression. In most patients, symptoms are neurologic, secondary to brachial plexus compression. The C8 and T1 nerve roots are involved in 90% of patients, producing pain and paresthesia in the ulnar nerve distribution (ie, the medial aspect of the arm and forearm and the ring and small fingers). Cervical nerve roots C5 through C7 are the second most commonly involved structures. Compression at these points produces pain in the radial nerve distribution within the arm, as well as in the neck, ear, upper chest, and upper back (7). Other neurologic symptoms include numbness, weakness, and cold intolerance. Neck pain, occipital headache, thenar wasting, and Raynaud phenomenon also may occur. Although neurogenic TOS is the most common type, it is the hardest to diagnose and treat (9).

Venous compression may cause subclavian vein thrombosis, which is manifested in arm swelling, distention of the superficial veins of the upper arm and shoulder region, cyanosis, and pain. Subclavian artery compression may cause mural thrombosis and aneurysmal dilatation with the risk of distal embolization and digital ischemia (Fig 1). Symptoms may include claudication, pallor, coldness, paresthesia, and pain in the arm and hand.

In most cases, the physical examination is normal. However, in the presence of arterial TOS, the distal pulse measurement may be abnormal, and there may be an asymmetric reduction of blood pressure in the affected arm by more than 20 mm Hg.

Diagnostic Evaluation

There is no specific examination that proves the diagnosis of TOS. Therefore, the condition is diagnosed in cases where clinical suspicion is high because of a combination of positive clinical and imaging findings.

Several provocative clinical tests can be performed when the presence of TOS is suspected. These include the Roos, Adson, and Wright tests, all of which are based on revelation of an abnormality in response to dynamic compression of the vessels. The Roos test is used to provoke symptoms with the patient repeatedly clenching and unclenching the fists while keeping the arms abducted and externally rotated. In the Adson test, the radial pulses are palpated while the patient is in a sitting position with hands on thighs, the neck hyperextended, and the head turned toward the affected side. Obliteration of the radial pulse during this maneuver is a positive sign of TOS. The Wright test is performed during hyperabduction of the arms; again, diminution of the pulse is considered a positive finding of TOS. However, the results of most such tests are considered unreliable, and the most consistently useful maneuver for the diagnosis of TOS is abduction or hyperabduction of the arm (4).

Radiologic Imaging

Radiography.—Radiography of the neck and chest may depict lower cervical and upper thoracic osseous abnormalities such as cervical ribs, an elongated transverse process of the C7 vertebra, an abnormal first rib or clavicle, or neoplastic or posttraumatic abnormalities in bone.

Doppler US.—Color duplex US can depict subclavian vessel thrombosis and dynamic vessel compression during arm maneuvers. The diagnosis of TOS at US is indirect and is based on alteration of blood flow (eg, complete cessation of flow, increased flow velocity as a sign of stenosis); the site of vessel compression is not demonstrated (10). B-mode scanning may be useful for diagnosis of arterial TOS, as it may allow detection of anatomic abnormalities such as aneurysmal dilatation and vessel deviation (11).

CT Angiography.—CT angiography is an excellent tool for demonstrating vascular and osseous abnormalities. Intravenous contrast material should be injected from the side opposite that of imaging, to avoid injection artifacts. The study should be performed with the arms first placed alongside the body (adducted) and then elevated above the head (hyperabducted). The two sets of images are then compared to assess the degree of vascular compression with the arms elevated (positional CT). The ideal protocol for the diagnosis of arterial TOS begins with the intravenous administration of 90 mL of contrast material at a rate of 4 mL/sec, with arterial phase imaging performed 15–20 seconds after and CT venography performed 80–90 seconds after the injection is initiated (5). Sagittal and coronal reconstructions and volume rendering are helpful for the diagnostic interpretation of imaging features. Venous compression may be difficult to diagnose because some degree of compression is frequently present in all compartments of the thoracic outlet in asymptomatic individuals when the arm is elevated (4,12).

CT angiography also facilitates the detection of collateral pathways of arterial and venous circulation in the presence of thrombosis or hemodynamically significant compression. The main limitations of the modality are its restricted capability for depicting the brachial plexus, the minimal arm abduction that can be performed inside the scanner gantry, and the fact that angiographic studies performed with the patient supine may lead to false-negative findings (12,13).

MR Angiography.—MR angiography should be performed with a phased-array body coil. MR imaging provides superior soft tissue contrast resolution, with the main advantage being portrayal of the brachial plexus, scalene muscle abnormalities, and fibrous bands. As in CT angiography, two studies are performed with the arm in different positions. A sagittal T1-weighted sequence is the optimal technique for depicting anatomic details and vascular and nervous compression (4). The main limitation of MR angiography, as of CT angiography, is the patient's restricted ability to elevate the arm when lying inside the magnet.

Conventional Angiography.—DSA (including both arteriography and venography) has therapeutic as well as diagnostic uses in patients with a vascular compression syndrome. Dynamic

extrinsic compression, thrombosis, and aneurysmal dilatation of vessels, along with the presence of distal emboli and collateral vessels, can be readily diagnosed with DSA. The main limitation of DSA is that the impinging anatomic musculoskeletal structure is not demonstrated clearly (1). The DSA examination includes venography of both limbs, because in 15% of patients with subclavian vein thrombosis both limbs are involved (14).

Management

Treatment algorithms depend on the type and severity of TOS. Accurate diagnosis of the underlying structural abnormality is necessary to prevent recurrence. Neurogenic TOS is usually treated conservatively with physical therapy, nonsteroidal anti-inflammatory agents, and muscle relaxants (1). In cases of acute thrombosis, the restoration of venous or arterial blood flow is accomplished with catheter-directed thrombolytic therapy and concomitant anticoagulation therapy, or with brachial artery thromboembolectomy. Since TOS is caused by extrinsic compression, symptomatic patients with or without thrombosis also benefit from surgery (1). Surgical strategies include resection of cervical and first ribs, with or without anterior scalenectomy, and lysis of any fibrous bands present.

Apart from restoring perfusion to the arm and decompressing the thoracic outlet space, any aneurysmal dilatation or stenosis of the artery may prompt reconstruction of the arterial segment, which is often the source of emboli (1).

Endoluminal stents should not be used in the initial management of TOS because subclavian vessel compression frequently results in stent bending, fracture, or rethrombosis; therefore, stent placement is reserved for use in patients with recurrent occlusion or postsurgical stenosis (15).

Paget-Schroetter Syndrome

Paget-Schroetter syndrome, also referred to as effort thrombosis, is a subtype of venous TOS caused by vigorous overhead arm physical activity and is most often seen in young athletic males. Annual incidence in the United States is estimated at one to two cases per 100,000 in the general population (15). The syndrome is characterized by primary thrombosis of the subclavian vein at the costoclavicular junction (15). The subclavian vein is subject to compression and injury where it passes through the costoclavicular space, between the first rib and the clavicle. Repetitive or vigorous activity can cause trauma to the vein and precipitate venous thrombosis (16) (Fig 2).

It is unclear whether Paget-Schroetter syndrome is secondary to narrowing of the costoclavicular space because of anterior scalene or subclavian muscle hypertrophy and osseous abnormality of the clavicle or first rib or whether it can occur spontaneously, without any other abnormality (15). Treatment of Paget-Schroetter syndrome is the same as that of any other type of TOS, with catheter-mediated thrombolysis in the acute disease setting and surgical decompression of the costoclavicular junction in a second therapeutic phase. The latter is necessary because thrombosis recurs in one-third of patients in whom the underlying anatomic problem is not surgically corrected (17).

Quadrilateral Space Syndrome

Quadrilateral space syndrome is a neurovascular compression syndrome involving the posterior humeral circumflex artery and/or the axillary nerve in the quadrilateral space (18) (Fig 4).

The quadrilateral space is the anatomic compartment formed by the teres major inferiorly, the long head of the triceps medially, the teres minor posteriorly, the subscapularis anteriorly, and the surgical neck of the humerus laterally. The most common causes of the clinical syndrome are posttraumatic fibrotic bands within the quadrilateral space that tend to compress the posterior humeral circumflex artery, and hypertrophy of the muscles in throwing athletes such as tennis players (20). However, the pathophysiology of quadrilateral space syndrome remains to be elucidated; it is not clear whether the compression is dynamic or static (18).

The syndrome usually occurs in physically active adults between the ages of 20 and 35 years. Symptoms may include point tenderness over the quadrilateral space, burning pain and paresthesias over the lateral aspect of the shoulder and arm, and weakness of the deltoid and teres minor muscles, all of which are usually aggravated during abduction and external rotation of the arm (18).

Physical examination should focus on identifying the location of point tenderness in the quadrilateral space. Atrophy of the deltoid and teres minor muscles also may be noted.

Imaging Evaluation

Conventional Angiography.—DSA should be performed with the arm in a neutral position as well as with the Lang maneuver (ie, hyperabduction and external rotation of the affected arm

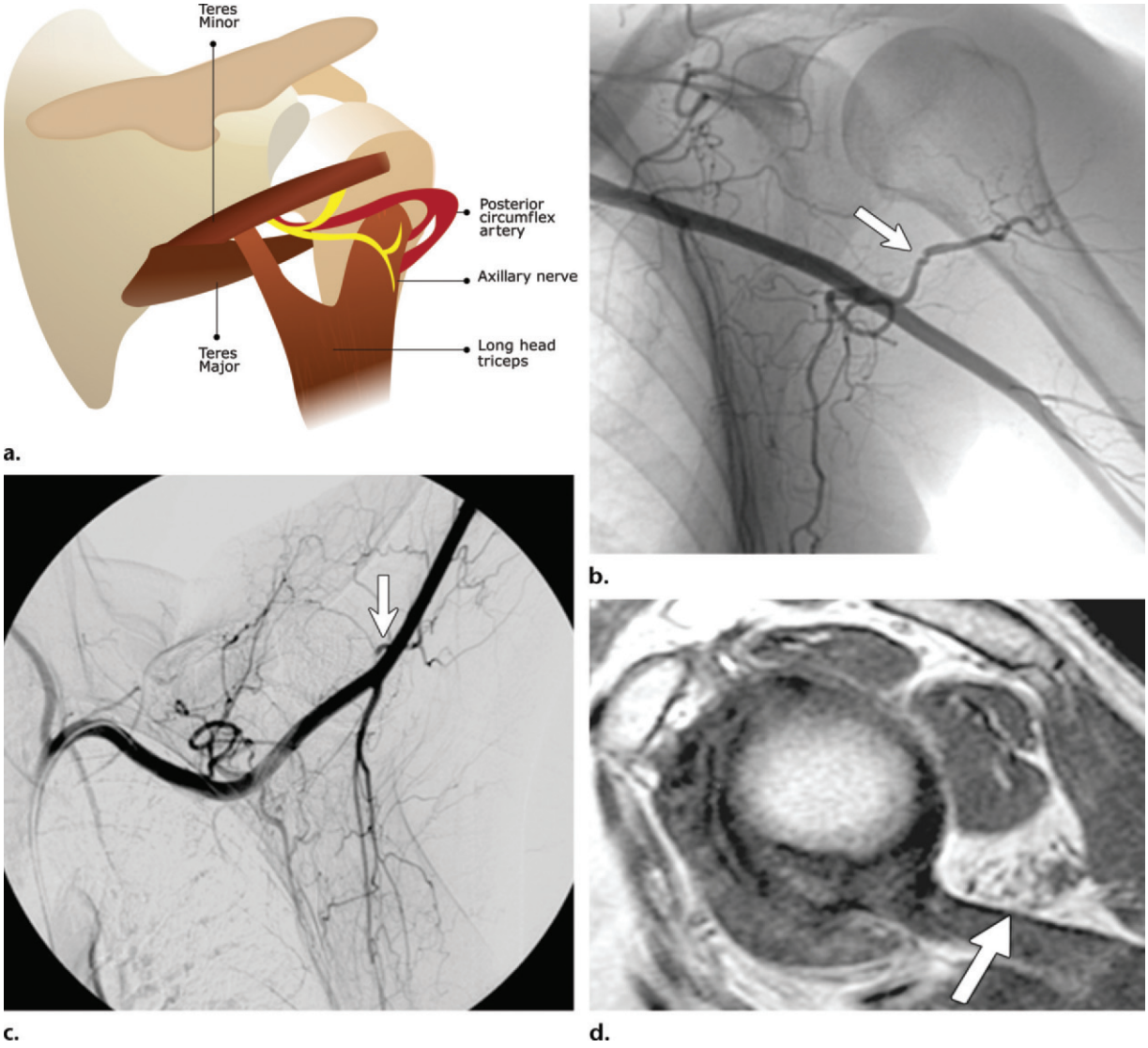

Figure 4. Quadrilateral space syndrome. **(a)** Drawing shows the complex anatomy of the quadrilateral space. **(b, c)** Quadrilateral space syndrome in a 55-year-old woman with chronic left shoulder pain, deltoid wasting, and an abnormal axillary nerve electromyogram. The patient's pain worsened during the Lang maneuver (with hyperabduction and external rotation of the arm while the head was turned contralaterally). Arteriogram obtained at DSA with the arm in a neutral position **(b)** shows a kink in the posterior circumflex humeral artery (arrow) caused by external compression. Arteriogram obtained at DSA during the Lang maneuver **(c)** shows occlusion of the posterior circumflex humeral artery (arrow). **(d)** Sagittal oblique T1-weighted MR image in another patient shows fatty atrophy of the teres minor muscle (arrow). (Fig 4d reprinted, with permission, from reference 19.)

with contralateral rotation of the head). The ipsilateral shoulder is raised, and a weight is placed in the hand. Occlusion of the posterior humeral circumflex artery in the dynamic position (21), the main finding of quadrilateral space syndrome, is considered diagnostic; however occlusion of the posterior humeral circumflex artery was also reported in 80% of asymptomatic control subjects in one study (22).

MR Imaging.—MR imaging may demonstrate a distinctive appearance of selective teres minor fatty atrophy (23) (Fig 4d). In addition, MR imaging can improve diagnostic specificity by helping rule out conditions such as rotator cuff tear and labral abnormality, which can cause

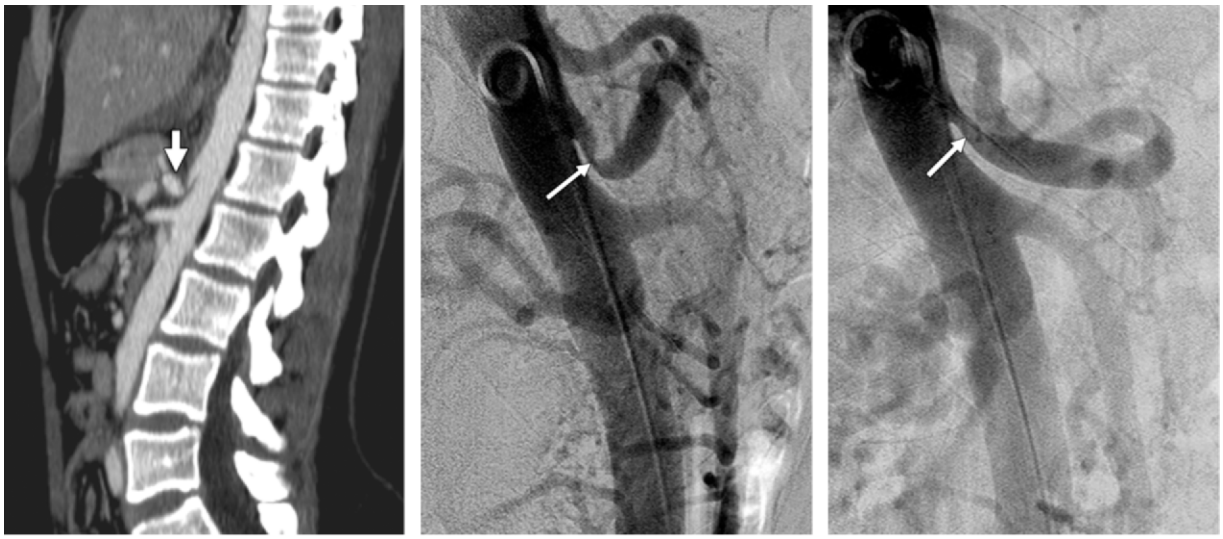

a. b. c.

Figure 5. Median arcuate ligament syndrome in a 45-year-old woman with postprandial abdominal pain, intermittent nausea, and weight loss. **(a)** Sagittal maximum intensity projection image obtained at contrast-enhanced CT shows the proximal celiac artery with acute upward angulation, abnormal indentation over its proximal aspect, and severe poststenotic dilatation (arrow). **(b)** Lateral superior mesenteric arteriogram obtained at DSA at end inspiration shows a severe, persistent focal stenosis (arrow) near its origin, with poststenotic dilatation and absence of filling of the common hepatic artery. **(c)** Lateral superior mesenteric arteriogram obtained at DSA during simple breath holding shows a marked reduction in the severity of the stenosis (arrow) but persistent poststenotic dilatation.

symptoms mimicking those of quadrilateral space syndrome (18). Hence, some authors favor MR imaging over DSA for the diagnosis of quadrilateral space syndrome (24).

Management

Initial treatment is usually conservative and includes analgesics, physiotherapy, and avoidance of athletic activities (18). Surgery is reserved for acute or chronic cases that fail to respond to conservative management and includes neurovascular release with resection of fibrous bands located in the quadrilateral space.

Median Arcuate Ligament Syndrome

Median arcuate ligament syndrome, also known as celiac artery compression syndrome, is caused by compression of the celiac artery by the median arcuate ligament. The median arcuate ligament is a fibrous arch that connects the diaphragmatic crura on both sides of the aortic hiatus. The ligament normally passes superior to the celiac axis at the level of the L1 vertebra. In 10%–24% of the general population, the ligament passes inferior and anterior to the celiac artery. In people with this anatomic variant, the proximal part of the celiac artery may be compressed by the abnormally low ligament, resulting in hemodynamically significant symptoms (25,26). Contributing anatomic factors may be a higher than normal celiac origin or lower than normal diaphragmatic crura.

Controversy surrounds the diagnosis of this syndrome, because imaging studies may yield false-positive findings in approximately half of normal subjects, and surgical treatment has had limited success in the past (25,27–29). Some authors deny the existence of this syndrome (28). Correlation of imaging findings with clinical findings is therefore crucial. Isolated compression of the celiac axis during end expiration is not necessarily a clinically significant event, and it may be observed in 10%–50% of normal subjects (25,29–31) (Fig 5).

The syndrome is most common in thin women who are between the ages of 20 and 40 years (25). Clinical features include postprandial epigastric pain, nausea, and weight loss. At physical examination, abdominal bruit that increases with expiration may be audible in the midepigastric region (25).

Imaging Evaluation

Conventional Angiography.—DSA performed with the patient in a lateral position has been the reference standard for diagnosis. The main find-

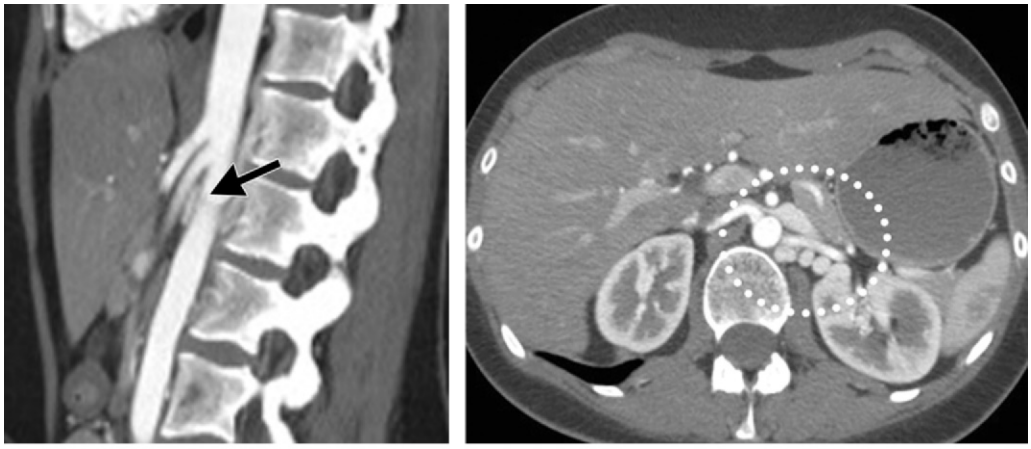

a. b.

Figure 6. Nutcracker syndrome in a 19-year-old woman with hematuria and left-sided flank pain. Sagittal **(a)** and axial **(b)** CT angiograms demonstrate compression of the left renal vein (arrow in **a**) between the aorta and superior mesenteric artery, with proximal venous dilatation and multiple perirenal collateral vessels (dotted circle in **b**).

ing is a characteristic superior indentation on the proximal celiac artery (25). When compression is suspected, imaging should be performed at expiration as well as end inspiration, when the celiac axis is in a more caudal position (30). Compression is considered severe when it persists at end inspiration, when it causes a poststenotic dilatation of the celiac artery, or when there is collateral filling of the celiac artery from the superior mesenteric artery and the pancreaticoduodenal arcade (25,29).

CT Angiography.—Angiography performed with thin-section multidetector CT, with sagittal reconstructions and maximum intensity projection images, may substitute for DSA for diagnosing median arcuate ligament syndrome. The main finding at CT angiography, as at DSA, is a characteristic focal narrowing ("hooked" appearance) of the proximal celiac artery on sagittal images obtained at expiration. The ligament is visible as it crosses the artery and may be thicker than usual (4 mm or more). A protocol suggested by Horton et al (25) begins with the injection of 120 mL of a nonionic contrast agent at a rate of 3 mL/sec, followed by arterial and venous phase scanning at 25 and 50 seconds after the injection with thin (0.75-mm) sections reconstructed every 0.5 mm for three-dimensional imaging.

MR Angiography.—MR angiography can also be useful for the diagnosis of median arcuate ligament syndrome. MR angiographic studies should be performed during inspiration and at end expiration (29).

Management

Laparoscopic surgery, with division of the median arcuate ligament and decompression of the celiac artery, has been performed with variable success; therefore it should be reserved for patients with classic and distinct findings such as postprandial pain, weight loss, poststenotic dilatation, and collateral vessels (32).

Nutcracker Syndrome

Teaching Point

Nutcracker syndrome (also known as renal vein entrapment syndrome) is caused by entrapment of the left renal vein between the superior mesenteric artery and the aorta, with resultant stenosis of the left renal vein leading to increased venous pressure, increased capillary pressure, and hematuria. A contributing factor may be a narrow angle of origin of the superior mesenteric artery from the aorta (33). The prevalence of nutcracker syndrome is unknown. It typically occurs in young, healthy individuals, mostly women in the 3rd–4th decade of life.

Intermittent asymptomatic gross hematuria is the usual manifestation (34). In men, reflux from the left renal vein to the left testicular vein may lead to a varicocele, left testicular pain, and infertility (35). In women, reflux to the ovarian vein may cause congestion in the ovarian and parametrial venous plexuses (36) and lead to pelvic congestion syndrome, which is characterized by genital, pelvic, and thigh varices, dysmenorrhea, dyspareunia, postcoital ache, and pelvic pain (37) (Fig 6).

Figure 7. May-Thurner syndrome. **(a)** Drawings show compression of the LCIV between the RCIA and the spine. **(b–h)** May-Thurner syndrome in a 44-year-old woman with a history of oral contraceptive use, a recent long flight, and left lower extremity swelling for 2 weeks before presentation. **(b)** Axial CT angiograms obtained with oral and intravenous contrast material at progressively lower levels (left to right) show compression of the LCIV by the RCIA (left, arrow), causing deep vein thrombosis in the LCIV (middle, arrow) and left common femoral vein (right, arrow). **(c, d)** Venograms obtained at DSA with the patient prone show deep vein thrombosis of the LCIV (arrow in **c**) and thrombosis of the superficial femoral and popliteal veins **(d)**. **(e)** Prone venogram obtained at DSA 24 hours after pharmacomechanical thrombolysis shows a critical stenosis of the distal LCIV at the RCIA crossover (arrow), a finding consistent with May-Thurner syndrome. **(f)** Supine venogram obtained at DSA after thrombolysis and LCIV stent placement (arrow) shows restoration of flow. The inferior vena cava filter was subsequently removed. **(g, h)** Photographs shows severe swelling, erythema, and edema of the left lower extremity at presentation **(g)** and a normal appearance 1 week after thrombolysis and LCIV stent placement **(h)**.

Imaging Evaluation

Doppler US.—Doppler imaging can be used to measure flow velocity and renal vein diameter at the renal hilum where the superior mesenteric artery crosses the renal vein (34,38). Flow velocity should exceed 100 cm/sec at this point (39). A sensitivity of 78% and specificity of 100% were reported with the use of Doppler US for diagnosis of nutcracker syndrome (38).

CT and MR Angiography.—Sagittal images from CT angiography and MR angiography demonstrate the renal venous anatomy between the superior mesenteric artery and the aorta and may show the precise compression point of the left renal vein. CT angiography and MR angiography also may depict dilated gonadal, periureteral, and perirenal veins, as well as pelvic venous collaterals (Fig 6).

Conventional Venography.—Retrograde left renal venography performed with DSA is the reference standard for the diagnosis of nutcracker syndrome. Compression of the left renal vein, reflux into the adrenal and gonadal veins, and the presence of periureteral and perirenal venous collaterals may be demonstrated. Venography also allows the measurement of increased blood pressure in the left renal vein and the renal venous–caval pressure gradient, with a gradient of more than 3 mm Hg being considered diagnostic of nutcracker syndrome. The renal venous–caval pressure gradient is an important diagnostic criterion because some degree of anatomic compression of the left renal vein between the aorta and the superior mesenteric artery is present in as many as 72% of subjects in the general population (40). It is important to correlate clinical and imaging findings because the anatomic configuration associated with the nutcracker syndrome is much more common than the clinical syndrome (41).

Management

The preferred method of treatment for nutcracker syndrome depends on the severity of symptoms. Most cases can be managed conservatively, especially those in young patients undergoing puberty, who have a higher rate of spontaneous remission (42). However, surgery may be necessary for severe cases with persistent hematuria. Several surgical techniques, including renal vein transposition, superior mesenteric artery reimplantation, renal autotransplantation, and gonadocaval bypass, may be applied, with the best outcomes reported for left renal vein transposition (41). Endovascular stent placement in the renal vein is an emerging minimally invasive alternative (43,44). In cases of severe pelvic congestion syndrome and varicocele, gonadal vein embolization or surgical ligation also may be effective (45).

May-Thurner (Cockett) Syndrome

Teaching Point

In May-Thurner or Cockett syndrome, the left common iliac vein (LCIV) is compressed between the right common iliac artery (RCIA) anteriorly and the fifth lumbar vertebra posteriorly. Chronic venous stasis resulting from compression may lead to deep vein thrombosis in the left iliac and femoral veins. The overlying RCIA may affect the LCIV in two ways: *(a)* by physically compressing it and *(b)* by producing intimal hypertrophy with synechiae due to repetitive pulsatile impact (46).

The syndrome is diagnosed in 2%–5% of people undergoing evaluation for chronic venous disorders (47). Most patients are women in the 2nd to 4th decades of life (48).

The most frequent symptom is left lower extremity swelling, which may or may not be due to deep vein thrombosis. Other symptoms include varicose veins, venous eczema, hyperpigmentation, exertional pain, and venous ulcers in the left leg. In some cases, pulmonary emboli may be the primary finding at presentation (49) (Fig 7).

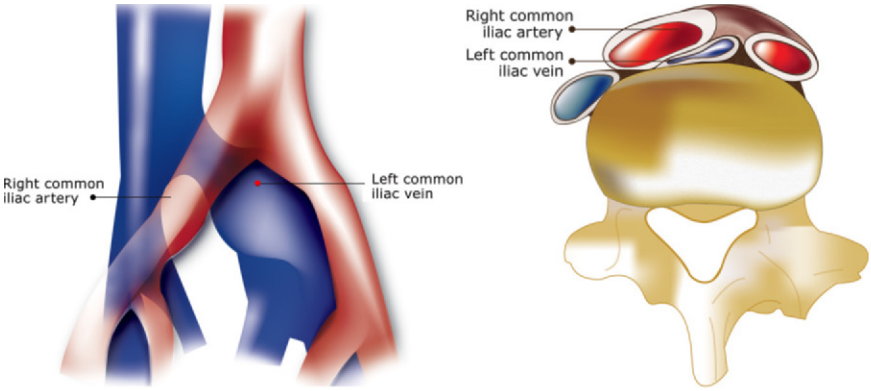
Right common iliac artery
Left common iliac vein
Right common iliac artery
Left common iliac vein

a.

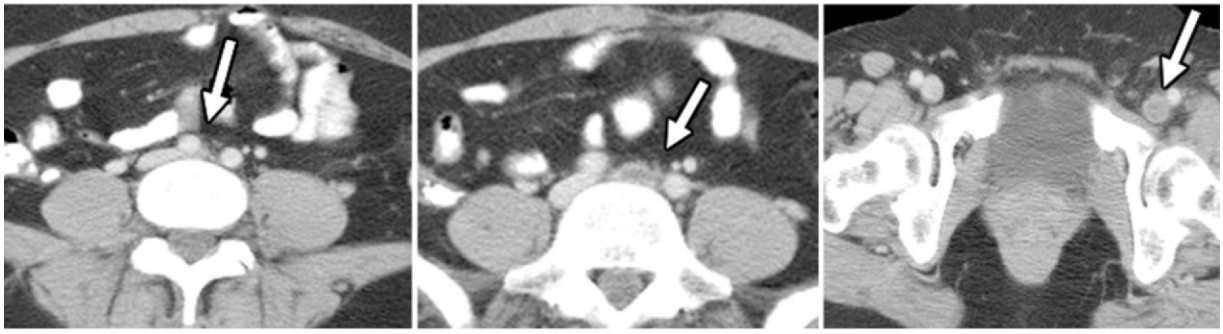

b.

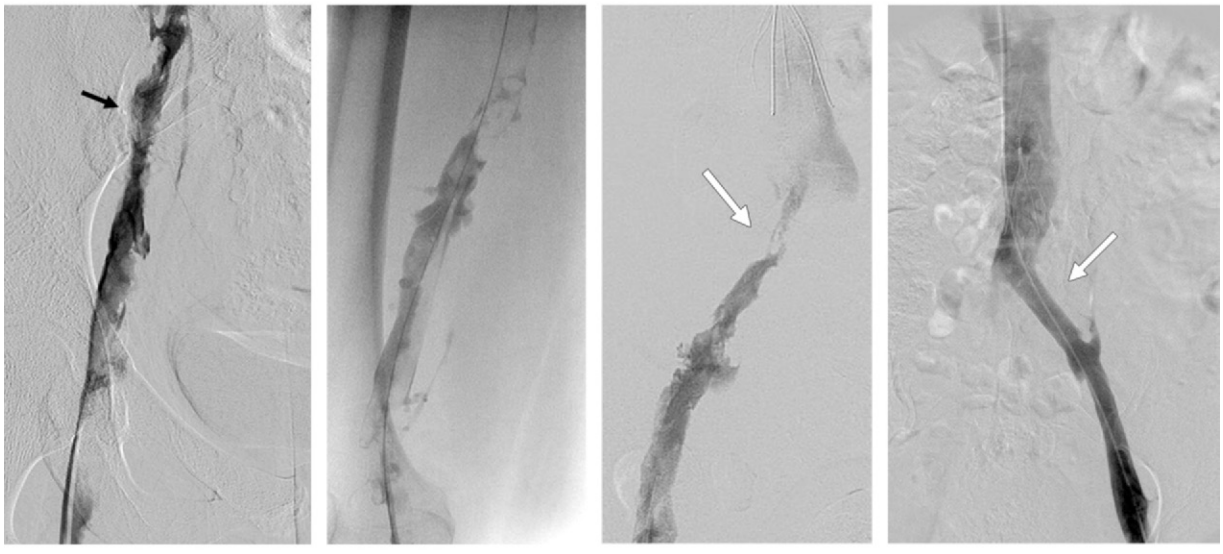

c. d. e. f.

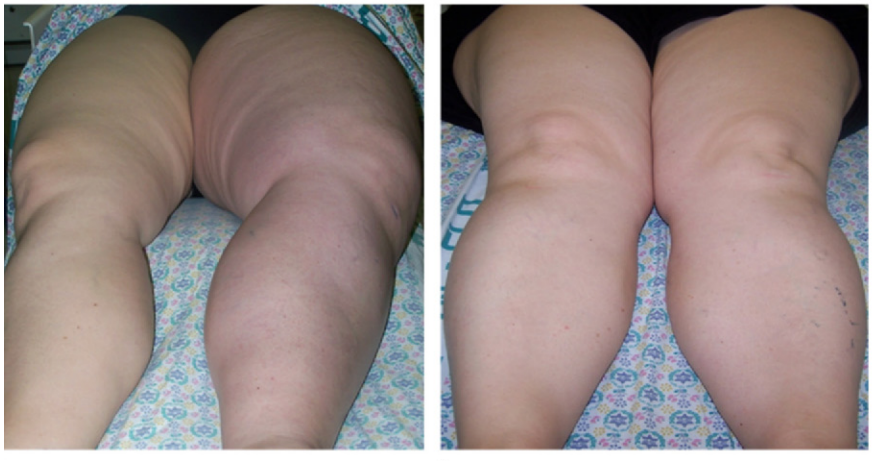

g. h.

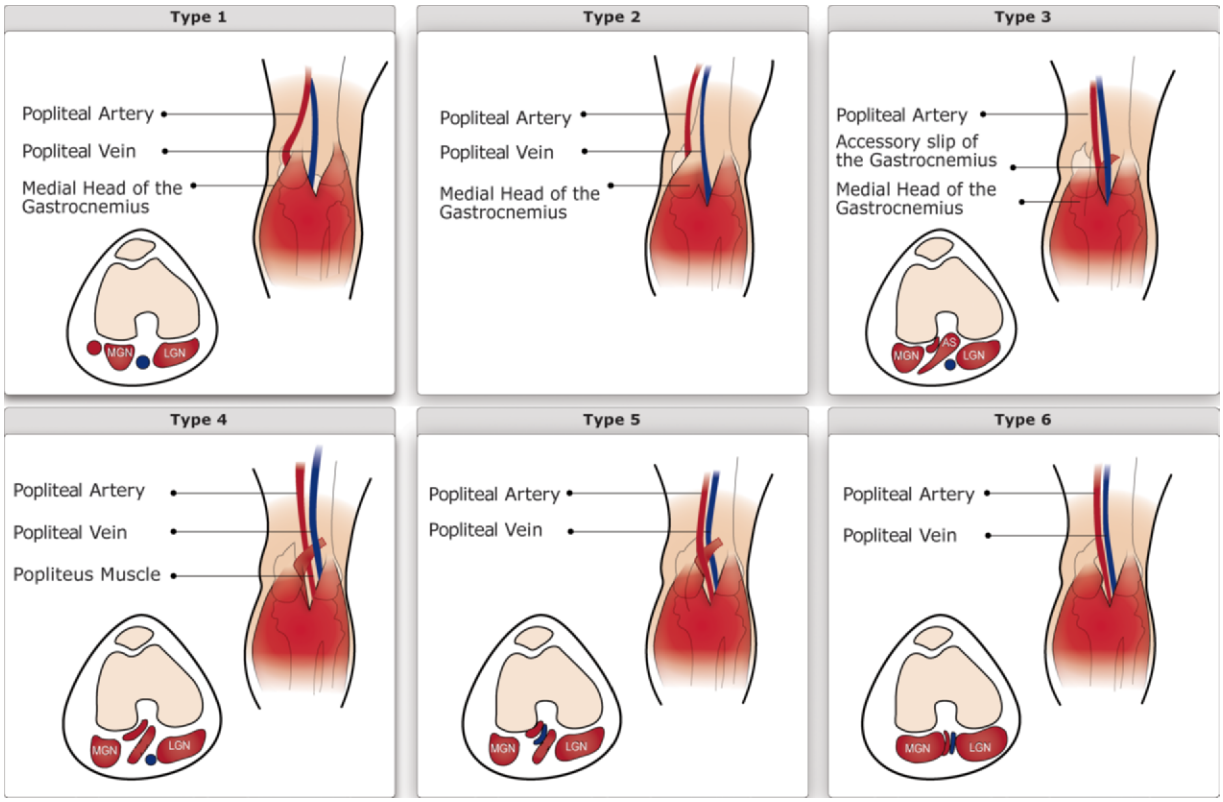

Figure 8. Schemas show the six types of popliteal artery entrapment syndrome. In type 1, the artery follows an aberrant medial course around the normal medial head of gastrocnemius muscle; in type 2, the artery is displaced medially by an abnormal head of the gastrocnemius muscle, which inserts laterally on the distal femur; in type 3, the normally positioned artery is enveloped and entrapped by an aberrant accessory slip from the medial head of the gastrocnemius muscle; in type 4, the artery is entrapped by its location deep in the popliteus muscle or beneath fibrous bands in the popliteal fossa; in type 5, the artery and vein are both entrapped; and in type 6, the functional, normally positioned artery is entrapped by a normally positioned but hypertrophic gastrocnemius muscle. *AS* = accessory slip, *LGN* = lateral gastrocnemius, *MGN* = medial gastrocnemius.

Imaging Evaluation

Doppler US.—Doppler US can depict deep vein thrombosis in the LCIV. However, the iliac vessels may not be adequately demonstrated by US in an estimated 20% of the general population (50).

Conventional Venography.—Retrograde venography performed with DSA is the reference standard for diagnostic imaging of patients in whom the presence of May-Thurner syndrome is suspected. Retrograde venography can show LCIV stenosis due to compression, and it allows quantitative assessment of the venous-caval pressure gradient. In addition, it may show tortuous venous collaterals crossing the pelvis and connecting with the contralateral veins (51).

MR Venography.—MR venography can demonstrate the venous course as well as the external compression and thrombosis frequently associated with May-Thurner syndrome. However, MR examination is expensive and time consuming and may be negatively affected by artifacts due to stents in the LCIV.

Anatomy-based Classification of Popliteal Artery Entrapment Syndromes

Syndrome Type	Underlying Anatomic Abnormality
1	Aberrant medial course of the popliteal artery around the normal medial head of the gastrocnemius muscle
2	Aberrant lateral insertion of the medial head of the gastrocnemius muscle on the distal femur, with resultant medial displacement of the popliteal artery
3	Abnormal accessory slip of gastrocnemius muscle
4	Fibrous band or popliteus muscle
5	Any abnormality causing entrapment of the popliteal vein as well as the artery
6	Hypertrophy of the gastrocnemius muscle

CT Venography.—CT venography is comparable to US for the diagnosis of femoropopliteal deep vein thrombosis (52) but is considered superior for the diagnosis of thrombosis of the iliac veins and inferior vena cava (53).

Management

Several surgical approaches have been used in the management of May-Thurner syndrome. Catheter-directed thrombolysis followed by angioplasty with stent placement in the iliac vein is an alternative that is used with increasing frequency (54) and recently was reported to provide long-term patency (55).

Popliteal Artery Entrapment Syndrome

Popliteal artery entrapment syndrome is a vascular compression syndrome of the popliteal artery, which usually courses between the two heads of the gastrocnemius muscle in the popliteal fossa. In popliteal artery entrapment syndrome, the artery is deviated from its normal course and is repeatedly compressed during plantar or dorsal flexion. Spontaneous thrombosis, distal embolization, and aneurysm formation may result (56,57).

Teaching Point

Six types of popliteal artery entrapment syndrome have been described on the basis of the anatomic abnormality causing entrapment (56,58–60) (Fig 8; Table). Type 3 popliteal artery entrapment syndrome is the most common, accounting for 30% of cases. Isolated compression of the popliteal vein has been reported rarely (61). Popliteal artery entrapment syndrome is most prevalent in healthy young males. An estimated 60% of patients are younger than 30 years, with a male-to-female ratio of 15:1 (62). The prevalence of popliteal artery entrapment syndrome is unknown. However, the syndrome was found in 0.165% of young males entering military service (63), and an associated anatomic abnormality was found in 3.8% of cadavers in a postmortem study (64); together, these results suggest that the anatomic anomaly may be much more common than the clinical syndrome. Popliteal artery entrapment syndrome is bilateral in 22%–67% of patients (65).

Claudication and exercise-induced leg pain, the most common symptoms at presentation, are seen in approximately 90% of patients. Approximately 10% of patients report symptoms of acute or chronic limb ischemia, including paresthesias, rest pain, or tissue loss, at presentation (66).

At physical examination, arterial compression during plantar flexion or dorsiflexion of the foot may cause a decrease in or disappearance of the normal pulses. In addition, the normal ankle-brachial index at rest may be decreased during exercise (56).

Some degree of narrowing of the popliteal artery with plantar flexion or dorsiflexion may occur in as many as 50% of the general population (67); therefore, it is crucial that radiologic imaging features be correlated with clinical manifestations before treatment is initiated (Fig 9).

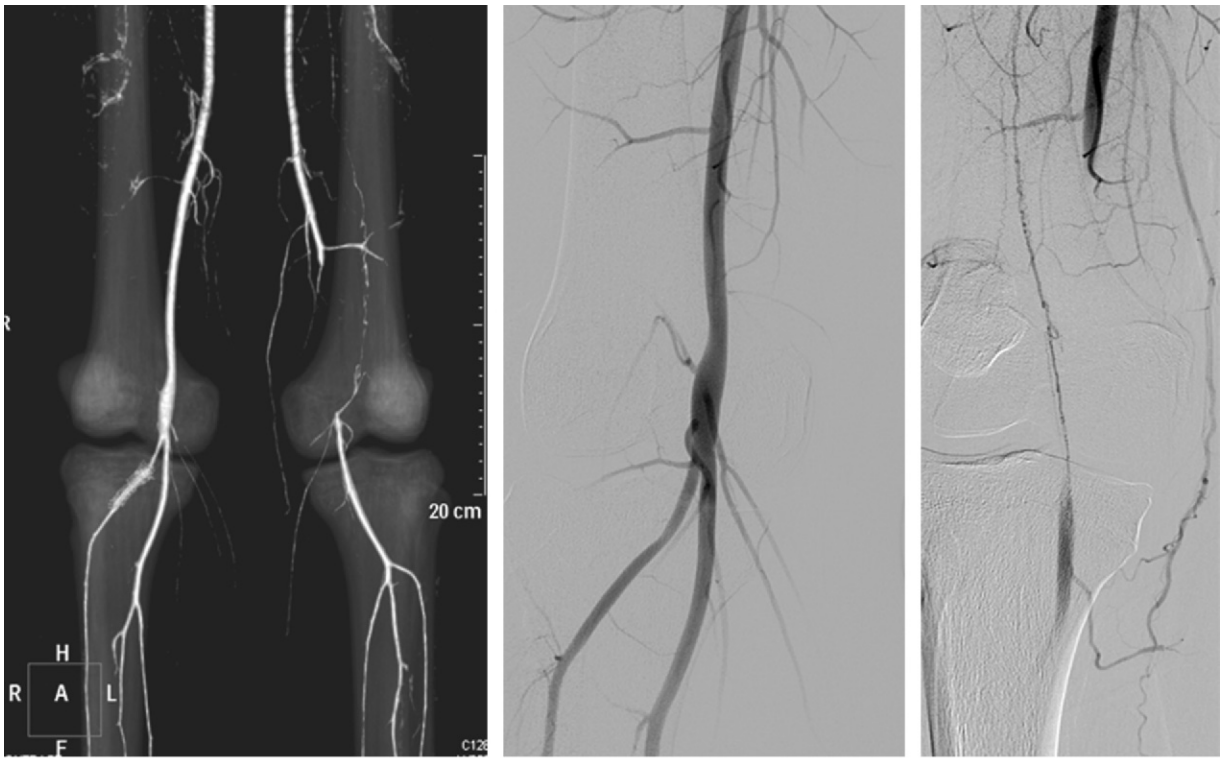

Figure 9. Popliteal artery entrapment syndrome in a healthy, athletic 30-year-old man with symptoms of claudication in both calves for several months. **(a)** Coronal three-dimensional CT angiogram obtained with the extremities in a neutral position shows complete obstruction of the left popliteal artery and aneurysmal dilatation of the right popliteal artery. **(b)** Arteriogram obtained at DSA depicts an aneurysm of the right popliteal artery and an abnormally high origin of the anterior tibial artery. **(c)** Arteriogram obtained at DSA during dorsiflexion of the right foot shows complete occlusion of the popliteal artery, helping confirm the diagnosis of popliteal artery entrapment syndrome.

Imaging Evaluation

Doppler US.—Doppler imaging may demonstrate popliteal artery stenosis, increased velocity, or decreased peak systolic activity, with dynamic compression (68). Popliteal artery occlusion during stress maneuvers can occur in as many as 88% of asymptomatic patients; hence, it is important to remember that there may be a significant false-positive rate with duplex Doppler US (69).

CT Angiography.—Because CT angiography is relatively noninvasive and provides excellent soft tissue contrast resolution and high spatial resolution, it may eventually replace DSA as the reference standard for diagnosis of popliteal artery entrapment syndrome (39,57). A standard CT angiography protocol for diagnosis of popliteal artery entrapment syndrome includes three separate intravenous injections of 60 mL of iodinated contrast material for scanning of the extremity with the foot in a neutral position, in plantar flexion, and in dorsal flexion. Axial scanning is performed from the middle calf to the middle thigh with a section thickness of 2 mm, increment of 1 mm, 120 kVp, and 200–300 mAs.

Multiplanar reconstructions, maximum intensity projections, and volume rendering are performed at image data reconstruction to aid the visualization of the entire vessel course and surrounding anatomy. Dynamic CT angiography is especially helpful in cases of advanced popliteal artery entrapment syndrome with thrombosis (57) (Movies 1, 2).

MR Angiography.—Like CT angiography, MR angiography is noninvasive and can demonstrate stenosis of the popliteal artery during dynamic compression. In addition, it has a superior capability for demonstrating the surrounding anatomy and soft tissue, helping determine the relation of the popliteal artery to the adjacent muscle in the popliteal fossa. Diagnostic accuracy with MR angiography has been reported to be comparable to that with DSA, with an absolute correlation of 95% between the two methods (70). The main limitation of MR angiography is its tendency to underestimate the degree of constriction in cases with stenosis of less than 50% in peripheral vessels because of the decreased spatial resolution and related volume averaging effects (39).

Conventional Angiography.—DSA is the standard imaging modality for detecting popliteal artery entrapment syndrome. DSA should be performed with the extremity in a neutral position as well as with dorsi- and plantar flexion during stress maneuvers. The main finding is narrowing of the popliteal artery during stress maneuvers. Both limbs should be examined because of the high percentage of bilateral disease. DSA also may show medial deviation, thrombosis, ectasia, aneurysm formation, vessel wall irregularity, and distal embolization to the tibial arteries. The disadvantage of DSA, apart from its invasiveness, is its inability to demonstrate the surrounding tissues.

Management

Catheter-mediated thrombolysis should be performed in patients with acute arterial thrombosis. However, the definitive treatment for popliteal artery entrapment syndrome of types 1 through 5 is surgical release of the gastrocnemius muscle. Once thrombosis or aneurysm develops in the artery, the damage is irreversible with decompression alone, and surgery must include vascular reconstruction (57).

Conclusions

Vascular compression syndromes are important clinical entities that usually affect young, otherwise healthy adults. They are often underdiagnosed because of a lack of physician awareness and the subtlety of clinical manifestations.

Because anatomic abnormalities that may cause intermittent vascular compression are more common than the vascular compression syndromes, the diagnosis of a syndrome should be based on correlation of clinical and radiologic findings. Endoluminal treatment is rarely adequate as the sole approach to management of a vascular compression syndrome. Since extrinsic compression is usually the cause of the syndrome, surgical decompression is required to achieve optimal and durable clinical benefits in most patients.

Acknowledgment.—The authors thank Shifra Fraifeld for her editorial assistance during the preparation of the manuscript.

Disclosures of Potential Conflicts of Interest.—**J.S.:** *Related financial activities:* none. *Other financial activities:* consultant for Activiews.

References

1. Demondion X, Herbinet P, Van Sint Jan S, Boutry N, Chantelot C, Cotten A. Imaging assessment of thoracic outlet syndrome. RadioGraphics 2006;26(6):1735–1750.
2. Davidovic LB, Kostic DM, Jakovljevic NS, Kuzmanovic IL, Simic TM. Vascular thoracic outlet syndrome. World J Surg 2003;27(5):545–550.
3. Fugate MW, Rotellini-Coltvet L, Freischlag JA. Current management of thoracic outlet syndrome. Curr Treat Options Cardiovasc Med 2009;11(2):176–183.
4. Demondion X, Bacqueville E, Paul C, Duquesnoy B, Hachulla E, Cotten A. Thoracic outlet: assessment with MR imaging in asymptomatic and symptomatic populations. Radiology 2003;227(2):461–468.
5. Remy-Jardin M, Remy J, Masson P, et al. Helical CT angiography of thoracic outlet syndrome: functional anatomy. AJR Am J Roentgenol 2000;174(6):1667–1674.
6. Sanders RJ, Hammond SL. Management of cervical ribs and anomalous first ribs causing neurogenic thoracic outlet syndrome. J Vasc Surg 2002;36(1):51–56.
7. Chang AK, Bohan JS. Thoracic outlet syndrome. eMedicine 2010. http://emedicine.medscape.com/article/760477-overview. Accessed January 13, 2011.
8. Atasoy E. Thoracic outlet compression syndrome. Orthop Clin North Am 1996;27(2):265–303.

9. Sharp WJ, Nowak LR, Zamani T, et al. Long-term follow-up and patient satisfaction after surgery for thoracic outlet syndrome. Ann Vasc Surg 2001;15 (1):32–36.
10. Wadhwani R, Chaubal N, Sukthankar R, Shroff M, Agarwala S. Color Doppler and duplex sonography in 5 patients with thoracic outlet syndrome. J Ultrasound Med 2001;20(7):795–801.
11. Demondion X, Vidal C, Herbinet P, Gautier C, Duquesnoy B, Cotten A. Ultrasonographic assessment of arterial cross-sectional area in the thoracic outlet on postural maneuvers measured with power Doppler ultrasonography in both asymptomatic and symptomatic populations. J Ultrasound Med 2006;25(2):217–224.
12. Matsumura JS, Rilling WS, Pearce WH, Nemcek AA Jr, Vogelzang RL, Yao JS. Helical computed tomography of the normal thoracic outlet. J Vasc Surg 1997;26(5):776–783.
13. Scherrer A, Roy P, Fontaine A. The compression syndrome: a revaluation of the value of postural angiography (author's transl) [in French]. J Radiol 1979;60(6-7):417–422.
14. Rosenbaum A, Silvis ML, Kalra A, Thornburg M, Spadone D. Thoracic outlet syndrome. eMedicine 2008. http://emedicine.medscape.com/article/96412-overview. Accessed January 13, 2011.
15. Illig KA, Doyle AJ. A comprehensive review of Paget-Schroetter syndrome. J Vasc Surg 2010;51 (6):1538–1547.
16. Shebel ND, Marin A. Effort thrombosis (Paget-Schroetter syndrome) in active young adults: current concepts in diagnosis and treatment. J Vasc Nurs 2006;24(4):116–126.
17. Urschel HC Jr, Razzuk MA. Paget-Schroetter syndrome: what is the best management? Ann Thorac Surg 2000;69(6):1663–1668; discussion 1668–1669.
18. Hoskins WT, Pollard HP, McDonald AJ. Quadrilateral space syndrome: a case study and review of the literature. Br J Sports Med 2005;39(2):e9.
19. Cothran RL Jr, Helms C. Quadrilateral space syndrome: incidence of imaging findings in a population referred for MRI of the shoulder. AJR Am J Roentgenol 2005;184(3):989–992.
20. Dugas JR, Weiland AJ. Vascular pathology in the throwing athlete. Hand Clin 2000;16(3):477–485, x.
21. Cahill BR, Palmer RE. Quadrilateral space syndrome. J Hand Surg Am 1983;8(1):65–69.
22. Mochizuki T, Isoda H, Masui T, et al. Occlusion of the posterior humeral circumflex artery: detection with MR angiography in healthy volunteers and in a patient with quadrilateral space syndrome. AJR Am J Roentgenol 1994;163(3):625–627.
23. Robinson P, White LM, Lax M, Salonen D, Bell RS. Quadrilateral space syndrome caused by glenoid labral cyst. AJR Am J Roentgenol 2000;175 (4):1103–1105.
24. Linker CS, Helms CA, Fritz RC. Quadrilateral space syndrome: findings at MR imaging. Radiology 1993;188(3):675–676.
25. Horton KM, Talamini MA, Fishman EK. Median arcuate ligament syndrome: evaluation with CT angiography. RadioGraphics 2005;25(5):1177–1182.
26. Lindner HH, Kemprud E. A clinicoanatomical study of the arcuate ligament of the diaphragm. Arch Surg 1971;103(5):600–605.
27. A-Cienfuegos J, Rotellar F, Valentí V, et al. The celiac axis compression syndrome (CACS): critical review in the laparoscopic era. Rev Esp Enferm Dig 2010;102(3):193–201.
28. Gloviczki P, Duncan AA. Treatment of celiac artery compression syndrome: does it really exist? Perspect Vasc Surg Endovasc Ther 2007;19(3):259–263.
29. Lee VS, Morgan JN, Tan AG, et al. Celiac artery compression by the median arcuate ligament: a pitfall of end-expiratory MR imaging. Radiology 2003;228(2):437–442.
30. Agnes S, Avolio AW, Magalini SC, Frongillo F, Castagneto M. Celiac axis compression syndrome in liver transplantation. Transplant Proc 2001;33 (1-2):1438–1439.
31. Bron KM, Redman HC. Splanchnic artery stenosis and occlusion: incidence; arteriographic and clinical manifestations. Radiology 1969;92(2):323–328.
32. Reilly LM, Ammar AD, Stoney RJ, Ehrenfeld WK. Late results following operative repair for celiac artery compression syndrome. J Vasc Surg 1985;2(1):79–91.
33. Hohenfellner M, Steinbach F, Schultz-Lampel D, et al. The nutcracker syndrome: new aspects of pathophysiology, diagnosis and treatment. J Urol 1991;146(3):685–688.
34. Kim SH, Cho SW, Kim HD, Chung JW, Park JH, Han MC. Nutcracker syndrome: diagnosis with Doppler US. Radiology 1996;198(1):93–97.
35. Pryor JL, Howards SS. Varicocele. Urol Clin North Am 1987;14(3):499–513.
36. Beard RW, Highman JH, Pearce S, Reginald PW. Diagnosis of pelvic varicosities in women with chronic pelvic pain. Lancet 1984;2(8409):946–949.
37. Beard RW, Reginald PW, Wadsworth J. Clinical features of women with chronic lower abdominal pain and pelvic congestion. Br J Obstet Gynaecol 1988;95(2):153–161.
38. Takebayashi S, Ueki T, Ikeda N, Fujikawa A. Diagnosis of the nutcracker syndrome with color Doppler sonography: correlation with flow patterns on retrograde left renal venography. AJR Am J Roentgenol 1999;172(1):39–43.

39. Kim HK, Shin MJ, Kim SM, Lee SH, Hong HJ. Popliteal artery entrapment syndrome: morphological classification utilizing MR imaging. Skeletal Radiol 2006;35(9):648–658.
40. Buschi AJ, Harrison RB, Norman A, et al. Distended left renal vein: CT/sonographic normal variant. AJR Am J Roentgenol 1980;135(2):339–342.
41. Wang L, Yi L, Yang L, et al. Diagnosis and surgical treatment of nutcracker syndrome: a single-center experience. Urology 2009;73(4):871–876.
42. Shin JI, Park JM, Kim JH, Lee JS, Jeong HJ. Factors affecting histological regression of crescentic Henoch-Schönlein nephritis in children. Pediatr Nephrol 2006;21(1):54–59.
43. Neste MG, Narasimham DL, Belcher KK. Endovascular stent placement as a treatment for renal venous hypertension. J Vasc Interv Radiol 1996;7(6):859–861.
44. Scultetus AH, Villavicencio JL, Gillespie DL. The nutcracker syndrome: its role in the pelvic venous disorders. J Vasc Surg 2001;34(5):812–819.
45. Tarazov PG, Prozorovskij KV, Ryzhkov VK. Pelvic pain syndrome caused by ovarian varices: treatment by transcatheter embolization. Acta Radiol 1997;38(6):1023–1025.
46. Heniford BT, Senler SO, Olsofka JM, Carrillo EH, Bergamini TM. May-Thurner syndrome: management by endovascular surgical techniques. Ann Vasc Surg 1998;12(5):482–486.
47. Taheri SA, Williams J, Powell S, et al. Iliocaval compression syndrome. Am J Surg 1987;154(2):169–172.
48. Cockett FB, Thomas ML. The iliac compression syndrome. Br J Surg 1965;52(10):816–821.
49. Kishi K, Homma S, Kawabata M, et al. Pulmonary emboli caused by iliac compression syndrome without leg symptoms. Respiration 2002;69(3):269–272.
50. Messina LM, Sarpa MS, Smith MA, Greenfield LJ. Clinical significance of routine imaging of iliac and calf veins by color flow duplex scanning in patients suspected of having acute lower extremity deep venous thrombosis. Surgery 1993;114(5):921–927.
51. Cil BE, Akpinar E, Karcaaltincaba M, Akinci D. Case 76: May-Thurner syndrome. Radiology 2004;233(2):361–365.
52. Yoshida S, Akiba H, Tamakawa M, Yama N, Takeda M, Hareyama M. Spiral CT venography of the lower extremities by injection via an arm vein in patients with leg swelling. Br J Radiol 2001;74(887):1013–1016.
53. Lim KE, Hsu WC, Hsu YY, Chu PH, Ng CJ. Deep venous thrombosis: comparison of indirect multidetector CT venography and sonography of lower extremities in 26 patients. Clin Imaging 2004;28(6):439–444.
54. Berger A, Jaffe JW, York TN. Iliac compression syndrome treated with stent placement. J Vasc Surg 1995;21(3):510–514.
55. Patel NH, Stookey KR, Ketcham DB, Cragg AH. Endovascular management of acute extensive iliofemoral deep venous thrombosis caused by May-Thurner syndrome. J Vasc Interv Radiol 2000;11(10):1297–1302.
56. Wright LB, Matchett WJ, Cruz CP, et al. Popliteal artery disease: diagnosis and treatment. RadioGraphics 2004;24(2):467–479.
57. Zhong H, Liu C, Shao G. Computed tomographic angiography and digital subtraction angiography findings in popliteal artery entrapment syndrome. J Comput Assist Tomogr 2010;34(2):254–259.
58. Rich NM, Collins GJ Jr, McDonald PT, Kozloff L, Clagett GP, Collins JT. Popliteal vascular entrapment: its increasing interest. Arch Surg 1979;114(12):1377–1384.
59. Rignault DP, Pailler JL, Lunel F. The "functional" popliteal entrapment syndrome. Int Angiol 1985;4(3):341–343.
60. Whelan TJ. Popliteal artery entrapment syndrome. In: Haimovici H, ed. Vascular surgery: principles and techniques. New York, NY: McGraw-Hill, 1976; 493–504.
61. Levien LJ. Popliteal artery entrapment syndrome. Semin Vasc Surg 2003;16(3):223–231.
62. Fowl RJ, Kempczinski RF. Popliteal artery entrapment. In: Rutherford RB, ed. Vascular surgery. 5th ed. Philadelphia, Pa: Saunders, 2000; 1987–1993.
63. Bouhoutsos J, Daskalakis E. Muscular abnormalities affecting the popliteal vessels. Br J Surg 1981;68(7):501–506.
64. Gibson MH, Mills JG, Johnson GE, Downs AR. Popliteal entrapment syndrome. Ann Surg 1977;185(3):341–348.
65. Collins PS, McDonald PT, Lim RC. Popliteal artery entrapment: an evolving syndrome. J Vasc Surg 1989;10(5):484–489; discussion 489–490.
66. Stager A, Clement D. Popliteal artery entrapment syndrome. Sports Med 1999;28(1):61–70.
67. Erdoes LS, Devine JJ, Bernhard VM, Baker MR, Berman SS, Hunter GC. Popliteal vascular compression in a normal population. J Vasc Surg 1994;20(6):978–986.
68. di Marzo L, Cavallaro A, Sciacca V, et al. Diagnosis of popliteal artery entrapment syndrome: the role of duplex scanning. J Vasc Surg 1991;13(3):434–438.
69. Hoffmann U, Vetter J, Rainoni L, Leu AJ, Bollinger A. Popliteal artery compression and force of active plantar flexion in young healthy volunteers. J Vasc Surg 1997;26(2):281–287.
70. Vavrik J, Rohrmoser GM, Madani B, Ersek M, Tscholakoff D, Bucek RA. Comparison of MR angiography versus digital subtraction angiography as a basis for planning treatment of lower limb occlusive disease. J Endovasc Ther 2004;11(3):294–301.

RadioGraphics

Between a Rock and a Hard Place: Clinical and Imaging Features of Vascular Compression Syndromes

Ruth Eliahou, MD • Jacob Sosna, MD • Allan I. Bloom, MD

RadioGraphics 2012; 32(1):E33–E49 • **Published online** 10.1148/rg.321115011 • **Content Codes:** IR VA

Page E34 (Figure 1 on page E34. Figure 2 on page E35)
There are three distinct types of TOS: neurogenic, arterial, and venous (Figs 1, 2), depending on what anatomic structure is compressed (2).

Page E36
Even with the arm at rest, anatomic anomalies may result in narrowing of the thoracic outlet, a condition that may be exacerbated during physical maneuvers such as abduction of the arm.

Page E41
Nutcracker syndrome (also known as renal vein entrapment syndrome) is caused by entrapment of the left renal vein between the superior mesenteric artery and the aorta, with resultant stenosis of the left renal vein leading to increased venous pressure, increased capillary pressure, and hematuria.

Page E42
In May-Thurner or Cockett syndrome, the left common iliac vein (LCIV) is compressed between the right common iliac artery (RCIA) anteriorly and the fifth lumbar vertebra posteriorly. Chronic venous stasis resulting from compression may lead to deep vein thrombosis in the left iliac and femoral veins.

Page E45
In popliteal artery entrapment syndrome, the artery is deviated from its normal course and is repeatedly compressed during plantar or dorsal flexion. Spontaneous thrombosis, distal embolization, and aneurysm formation may result (56,57).